Finite-size corrections to scaling of the magnetization distribution in the two-dimensional XY model at zero temperature

G. Palma,[1,*] F. Niedermayer,[2] Z. Rácz,[3] A. Riveros,[1] and D. Zambrano[4]

[1]*Departamento de Física, Universidad de Santiago de Chile, Casilla 307, Santiago 2, Chile*

[2]*Albert Einstein Center for Fundamental Physics, Institute for Theoretical Physics, University of Bern, Switzerland*

[3]*MTA-ELTE Theoretical Physics Research Group, Budapest, Hungary*

[4]*Departamento de Física, Universidad Técnica Federico Santa María, Avenida España 1680, Casilla 110-V, Valparaíso, Chile*

(Received 5 April 2016; revised manuscript received 18 July 2016; published 29 August 2016)

The zero-temperature, classical XY model on an $L \times L$ square lattice is studied by exploring the distribution $\Phi_L(y)$ of its centered and normalized magnetization y in the large-L limit. An integral representation of the cumulant generating function, known from earlier works, is used for the numerical evaluation of $\Phi_L(y)$, and the limit distribution $\Phi_{L\to\infty}(y) = \Phi_0(y)$ is obtained with high precision. The two leading finite-size corrections $\Phi_L(y) - \Phi_0(y) \approx a_1(L)\,\Phi_1(y) + a_2(L)\,\Phi_2(y)$ are also extracted both from numerics and from analytic calculations. We find that the amplitude $a_1(L)$ scales as $\ln(L/L_0)/L^2$ and the shape correction function $\Phi_1(y)$ can be expressed through the low-order derivatives of the limit distribution, $\Phi_1(y) = [\, y\,\Phi_0(y) + \Phi_0'(y)\,]'$. Thus, $\Phi_1(y)$ carries the same universal features as the limit distribution and can be used for consistency checks of universality claims based on finite-size systems. The second finite-size correction has an amplitude $a_2(L) \propto 1/L^2$ and one finds that $a_2\,\Phi_2(y) \ll a_1\,\Phi_1(y)$ already for small system size ($L > 10$). We illustrate the feasibility of observing the calculated finite-size corrections by performing simulations of the XY model at low temperatures, including $T = 0$.

DOI: 10.1103/PhysRevE.94.022145

I. INTRODUCTION

Studies of the scaling properties of fluctuations have played an important role in developing the theory of equilibrium critical phenomena, and they also proved to be instrumental in exploring systems driven far from equilibrium where fluctuations often diverge in the thermodynamic limit. In particular, finding critical exponents through finite-size (FS) scaling has become a standard method for establishing universality classes [1–3] and, furthermore, the shapes of the distribution functions of fluctuations have also been used as hallmarks of universality classes for both equilibrium [4–7] and nonequilibrium systems [8–12].

One of the most studied distributions of critical order-parameter fluctuations is that of the two-dimensional (2D) classical XY model. The model is important in itself since it serves as a prime example of an equilibrium phase transition with topological order [13,14]. Recent interest comes also from a suggestion that its critical magnetization distribution, $P_L(m)$, may describe the fluctuations in a remarkable number of diverse far-from-equilibrium steady states. Examples range from the energy dissipation in turbulence [9,10] and interface fluctuations in surface evolution [8,12] to electroconvection in liquid crystals [15], as well as to river-height fluctuations [16]. In some of the examples, such as the surface growth problems described by the Edwards-Wilkinson model [17], one can establish a rigorous link to the low-temperature limit (spin-wave approximation) of the XY model. Furthermore, the non-Gaussian features of $P_L(m)$ such as its exponential and double exponential asymptotes appear to have generic origins [18,19], thus explaining the observed collapse in a remarkable set of experimental and simulation data. In the majority of the examples, however, the experiments or simulations provide data of insufficient accuracy to decide unambiguously about the universality class. Indeed, it is not easy even to observe the changes occurring in $P_L(m)$ if the XY model is considered at finite temperatures where the spin-wave approximation breaks down [20–22].

In order to be more confident about universality claims, one would like to be able to examine the distribution functions in more details. A well-known and much investigated method of extracting additional information in critical systems such as the zero-temperature XY model is the study of the FS behavior [1–3]. The implication of FS scaling is that the appropriately scaled distribution function has a well-defined limit when the system size tends to infinity ($L \to \infty$). A frequently used scaling variable is the centered and normalized magnetization $y = (m - \langle m\rangle)/\sigma_m$, where $\sigma_m^2 = \langle m^2\rangle - \langle m\rangle^2$. This choice of scaling variable eliminates possible divergences in $\langle m\rangle$ and, in general, produces a nondegenerate limit distribution $\Phi_0(y)$ [23]:

$$\lim_{L\to\infty} \Phi_L(y) \equiv \lim_{L\to\infty} \sigma_m\, P_L(\langle m\rangle + \sigma_m y) = \Phi_0(y). \quad (1)$$

The function $\Phi_L(y)$ can be expressed in a compact form for the zero-temperature XY model [24]. Its large-L limit, $\Phi_0(y)$, has been numerically evaluated and compared with simulations and experiments on a variety of systems (see, e.g., [9,16,18]).

Once the limit distribution is known, one can investigate the approach to $\Phi_0(y)$ as the system size increases. As we show below, keeping the leading and the next-to-leading terms, the FS corrections, $\delta\Phi_L(y) = \Phi_L(y) - \Phi_0(y)$, to the limit distribution can be written as

$$\delta\Phi_L(y) = a_1(L)\Phi_1(y) + a_2(L)\Phi_2(y) + O(\ln^2 L/L^4). \quad (2)$$

We kept two terms since the asymptotic L dependence of the leading term differs from the next one only by a slowly

*guillermo.palma@usach.cl

varying logarithmic factor. Indeed, our calculation yields the amplitudes $a_i(L)$ in the following form:

$$a_1(L) = \frac{\alpha \ln L + \gamma}{L^2} = \frac{\alpha \ln(L/L_0)}{L^2}, \quad a_2(L) = \frac{\gamma'}{L^2}. \tag{3}$$

Here the coefficient α of the logarithmic term can be expressed through the Catalan constant G as $\alpha = 3\pi/4G = 2.572\ldots$. The coefficients of the $1/L^2$ terms are $\gamma = -2.803$ (giving $L_0 = 2.973$) and $\gamma' = 2\pi/3$ (for details, see Sec. III).

A remarkable result about the function $\Phi_1(y)$ characterizing the leading shape correction to the limit distribution is that it can be expressed through $\Phi_0(y)$ as

$$\Phi_1(y) = [\, y\, \Phi_0(y) + \Phi_0'(y)\,]', \tag{4}$$

where the prime denotes the derivative with respect to y. The second scaling function $\Phi_2(y)$ is more complex in the sense that it cannot be expressed through a finite sum of the derivatives of the limit distribution. However, it can be calculated efficiently using integral representations as explained in Sec. III [see Eq. (24)] and in Appendix B [see Eq. (B18)].

Evaluating the scaling functions $\Phi_i(y)$ numerically, one observes that $a_1(L)\Phi_1(y) \gg a_2(L)\Phi_2(y)$ already for small systems ($L > 10$). As a consequence, the FS corrections to the limit distribution can be written to an excellent accuracy in the following form:

$$\delta\Phi_L(y) \approx \alpha \frac{\ln(L/L_0)}{L^2}[y\Phi_0(y) + \Phi_0'(y)\,]'. \tag{5}$$

The above expression can be easily calculated and compared with experiments and simulations using both scaling of the amplitude and checking the shape of the correction.

It is important to note that $\Phi_1(y)$ is uniquely determined by the limit distribution; thus, the leading shape correction has the same universality attributes as the limit distribution itself. In renormalization group language, the meaning of the above result is that the eigenfunction corresponding to the direction of slowest approach to the fixed point distribution can be expressed through the limit distribution. A simple and transparent derivation of an analogous result for the case of the central limit theorem can be found in [25].

In order to show the workings of the method of FS scaling, we carried out Monte Carlo (MC) simulations of the XY model in its low-temperature limit, including its $T = 0$ limit. We examined the FS corrections described above for the lattice of size $L = 10$, as an illustration, and found close agreement between theoretical and MC results.

The paper is organized as follows. The XY model and the zero-temperature magnetization distribution are described in Sec. II. Next, the FS corrections are calculated in Sec. III, with the technicalities relegated to two appendixes (the direct calculations of the needed cumulants are found in Appendix A, while an integral representation that simplifies the evaluation of finite-volume sums is presented in Appendix B). Finally in Sec. IV, and as an illustration, we have compared the FS results with the MC simulations for a lattice of size $L = 10$.

II. PROBABILITY DENSITY OF THE MAGNETIZATION FOR THE CLASSICAL XY MODEL IN TWO DIMENSIONS

The two-dimensional, classical XY model on a square lattice is defined by the Hamiltonian

$$H = -\sum_{\langle i,j\rangle} \cos(\theta_i - \theta_j), \tag{6}$$

where the angle variables θ_i are located at the lattice sites and describe the orientation of unit vectors in the plane. The energy and the length scales in the problem are defined by setting both the ferromagnetic interaction strength and the lattice spacing to unity.

The order parameter m whose probability distribution is of our interest is defined as

$$m = \frac{1}{L^2}\sum_i \cos(\theta_i - \bar\theta), \tag{7}$$

where $\bar\theta$ is the instantaneous average orientation. The probability density function (PDF) of the magnetization, $P_L(m)$, has been much studied [9,16,18–22,24]. Its zero-temperature limit ($T \to 0$) has been first calculated [24] by using the spin-wave approximation $\cos(\theta_i - \theta_j) \approx 1 - (\theta_i - \theta_j)^2/2$ and summing up the moments series for the PDF.

Another, field-theoretic, approach for obtaining $P_L(m)$ is based on evaluating the Fourier transform of the partition function of the system in a loop expansion [20]. It turns out that the n-loops contribution corresponds to the T^{n-1} contribution, where T is the system temperature. Correspondingly, the expansion up to one-loop gives exactly the zero-temperature limit of $P_L(m)$.

Both of the above methods yield an identical result to leading order. The second method, however, shows explicitly how to compute the higher-temperature corrections to $P_L(m)$ through an effective, T-dependent lattice propagator, $\Gamma = (I + \frac{ikT}{L^2}\mathcal{G})^{-1}\mathcal{G}$, where $\mathcal{G}$ is independent of T [26], and is defined by its Fourier representation as

$$\mathcal{G}(\mathbf{k}) = 1/\hat{\mathbf{k}}^2. \tag{8}$$

Here the components of the vector $\hat{\mathbf{k}}$ are $\hat k_i = 2\sin(k_i/2)$, where $k_i = 2\pi n_i/L$, with $i = 1,2$ and $n_i \in Z$ such that the lattice momentum $\mathbf{k}$ lies in the first Brillouin zone: $-\pi < k_i \leqslant \pi$.

Hence, the PDF at $T = 0$ can be obtained by the well-known "1/2 Trace(ln)" expression of the one-loop result [20],

$$\Phi_L(y) = \int_{-\infty}^{\infty} \frac{dq}{2\pi}\sqrt{\frac{g_2}{2}}\exp\left(i\sqrt{\frac{g_2}{2}}qy\right) \times \exp\left(-\frac{1}{2}\sum_{\mathbf{k}\neq 0}\left\{\ln\left[1 - \frac{iq}{L^2}\mathcal{G}(\mathbf{k})\right] + \frac{iq}{L^2}\mathcal{G}(\mathbf{k})\right\}\right), \tag{9}$$

where y is the centered and normalized magnetization $y = (m - \langle m\rangle)/\sigma_m$, and the coefficient g_2 is defined as the particular $n = 2$ case of the general expression:

$$g_n \equiv g_n(L) = \sum_{\mathbf{k}\neq 0} \mathcal{G}(\mathbf{k})^n/L^{2n}. \tag{10}$$

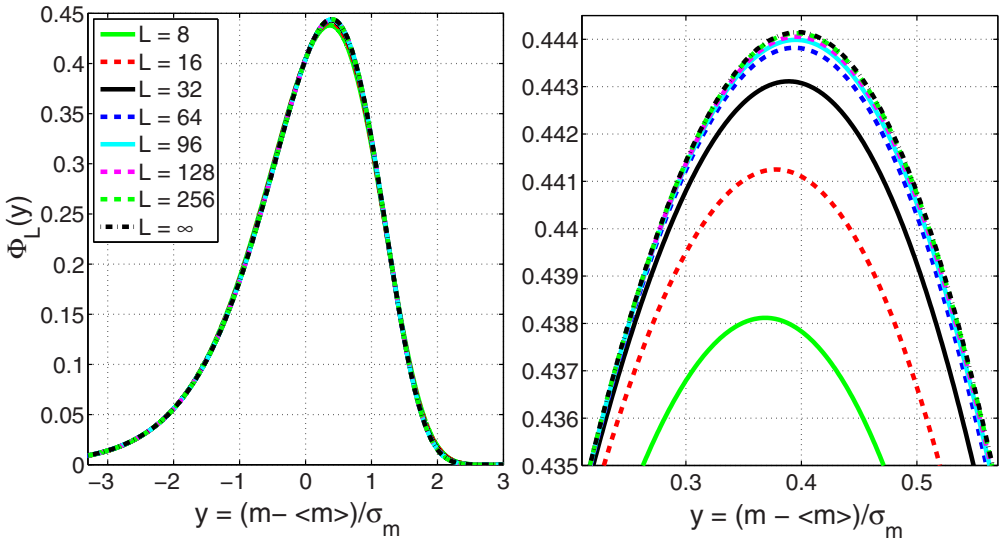

FIG. 1. The scaled probability density of the magnetization $\Phi_L(y)$, computed numerically using Eq. (9), is displayed for various lattice sizes L. The remarkably fast convergence to the limit distribution $\Phi_0(y)$ is demonstrated in the left panel, while, to illustrate the corrections to the limit distribution, the peak region of the $\Phi_L(y)$ is magnified in the right panel.

The PDF in Eq. (9) agrees with the corresponding formula obtained in [18] [see Eq. (26) therein].

In Fig. 1 we plot $\Phi_L(y)$ as a function of y using Eq. (9) for different L values. On the right panel, we display a magnification into the region close to the peak of the distribution functions. It can be clearly seen that $\Phi_L(y)$ tends towards an asymptotic distribution $\Phi_0(y)$ as $L \to \infty$ and, furthermore, one observes that the convergence is fast. Nevertheless, in experiments, the value of L is not known and deviations from $\Phi_0(y)$ are observed. They are often explained away as finite-size effects and thus leaving the universality claims not entirely justified. We would like to emphasize that there is information in the FS corrections (shown on Fig. 1 around the peak of the PDF) and, by evaluating these corrections, one may refine the reasoning for or against finding a universality class.

III. FINITE-SIZE CORRECTIONS TO THE LIMIT DISTRIBUTION

As explained in Sec. II, the PDF of the magnetization for the 2D XY model at $T = 0$ is given by the one-loop analytic expression of Eq. (9), and the numerical evaluation of the $L \to \infty$ limit distribution, $\Phi_0(y)$, can be carried out with an excellent precision. The aim of this section is to present the steps of the calculation of the leading and next-to-leading FS corrections to the limit distribution.

We start by expanding the logarithm in the exponential on the right-hand side of Eq. (9), which allows rewriting the equation in terms of the coefficients g_n defined by Eq. (10). After rescaling the integration variable by $\sqrt{g_2/2}$, we obtain $\Phi_L(y)$ as the Fourier integral

$$\Phi_L(y) = \int_{-\infty}^{\infty} \frac{dk}{2\pi} \exp\left\{iky - \frac{1}{2}k^2 + F_L(k)\right\}, \qquad (11)$$

where we have defined

$$F_L(k) = \sum_{n\geqslant 3} \frac{g_n}{2n}\left(ik\sqrt{\frac{2}{g_2}}\right)^n. \qquad (12)$$

The L dependence of the above sum is in the coefficients g_n, which have a finite nonzero thermodynamic limit $g_n(L \to \infty) = g_n^\infty$ for $n \geqslant 2$. Thus, in order to compute the FS behavior of $\Phi_L(y)$, we have to determine the FS corrections to g_n^∞,

$$g_n = g_n^\infty + \delta g_n. \qquad (13)$$

Assuming that δg_n is known, we can write $F_L(k)$ as

$$F_L(k) = F_0(k) + \delta F_1(k) + \delta F_2(k), \qquad (14)$$

where $F_0(k)$ is the thermodynamic limit of $F_L(k)$,

$$F_0(k) = \sum_{n\geqslant 3} \frac{g_n^\infty}{2n}\left(ik\sqrt{\frac{2}{g_2^\infty}}\right)^n \qquad (15)$$

and the FS corrections, due to δg_2 and δg_n for $n \geqslant 3$, are written separately:

$$\delta F_1(k) = -\frac{\delta g_2}{2g_2^\infty}\sum_{n\geqslant 3} \frac{g_n^\infty}{2}\left(ik\sqrt{\frac{2}{g_2^\infty}}\right)^n, \qquad (16)$$

$$\delta F_2(k) = \sum_{n\geqslant 3} \frac{\delta g_n}{2n}\left(ik\sqrt{\frac{2}{g_2^\infty}}\right)^n. \qquad (17)$$

The separation of the δg_2 and the $\delta g_{n\geqslant 3}$ contributions is partly motivated by their $L \to \infty$ asymptotic behaviors. It is shown in the appendixes that $\delta g_2 \sim \ln L/L^2$, while for $n \geqslant 3$, $\delta g_n \sim 1/L^2$. Thus, the leading correction comes from $\delta F_1(k)$ and the sum in Eq. (16) determines the shape (the functional form) of the leading correction. As it turns out, the same shape correction can be easily separated from the δg_n contributions for $n \geqslant 3$. Indeed, for large n, one has $\delta g_n \sim n g_n^\infty$, and one

can write [cf. Eqs. (A6), (B4), and (B15)]

$$\delta g_n = \frac{\pi^2}{3L^2} n g_n^\infty + \frac{2\pi}{3L^2} c_n, \tag{18}$$

where the second term is suppressed relative to the first one by a factor 4^{-n}. Substituting the above split of δg_n into Eq. (17), one can see the emergence of the same sum as in Eq. (16), and it allows us to write

$$\delta F_1(k) + \delta F_2(k) = a_1(L)\Psi_1(k) + a_2(L)\Psi_2(k), \tag{19}$$

where the L-dependent amplitudes are given by

$$a_1(L) = \frac{\delta g_2(L)}{2 g_2^\infty} - \frac{\pi^2}{3L^2}, \qquad a_2(L) = \frac{2\pi}{3L^2}, \tag{20}$$

while the corresponding L-independent functions by

$$\Psi_1(k) = -\sum_{n\geqslant 3} \frac{g_n^\infty}{2} \left(ik \sqrt{\frac{2}{g_2^\infty}} \right)^n = -k \frac{d}{dk} F_0(k),$$
$$\Psi_2(k) = \sum_{n\geqslant 3} \frac{c_n}{2n} \left(ik \sqrt{\frac{2}{g_2^\infty}} \right)^n. \tag{21}$$

Integral representations for $F_0(k)$ and $\Psi_2(k)$ are given in Eqs. (B5) and (B18), respectively, in Appendix B.

Inserting Eq. (19) into Eq. (11), we obtain the PDF of the 2D XY model at zero temperature, including its leading FS corrections:

$$\Phi_L(y) = \Phi_0(y) + a_1(L)\,\Phi_1(y) + a_2(L)\,\Phi_2(y). \tag{22}$$

Here

$$\Phi_0(y) = \int_{-\infty}^{\infty} \frac{dk}{2\pi} \exp\left\{ iky - \frac{k^2}{2} + F_0(k) \right\}, \tag{23}$$

and

$$\Phi_{1,2}(y) = \int_{-\infty}^{\infty} \frac{dk}{2\pi} \exp\left\{ iky - \frac{k^2}{2} + F_0(k) \right\} \Psi_{1,2}(k). \tag{24}$$

Since $\Psi_1(k) = -kF_0'(k)$, one can evaluate $\Phi_1(y)$ through $\Phi_0(y)$ by carrying out the appropriate integrations by part on the right-hand side of Eq. (24). The outcome is the leading shape correction expressed in terms of the limit distribution [as quoted in Eq. (4)]:

$$\Phi_1(y) = [\, y\,\Phi_0(y) + \Phi_0'(y)]'. \tag{25}$$

The second shape correction $\Phi_2(y)$ cannot be related to $\Phi_0(y)$ in such a simple manner but can be readily evaluated using Eqs. (24) and (B18) of the Appendix B.

The functions $\Phi_1(y)$ and $\Phi_2(y)$ are displayed in Fig. 2. A general property of these functions is that their zeroth, first, and second moments are zero. This follows from their definition as being corrections to a centered and normalized probability distribution and can be explicitly verified using their definitions, e.g., Eq. (24).

In order to determine the amplitudes in front of the shape corrections, we have to calculate the FS behavior of δg_n for $n \geqslant 2$. This problem is addressed in detail, using two distinct methods, in Appendixes A and B. It is found

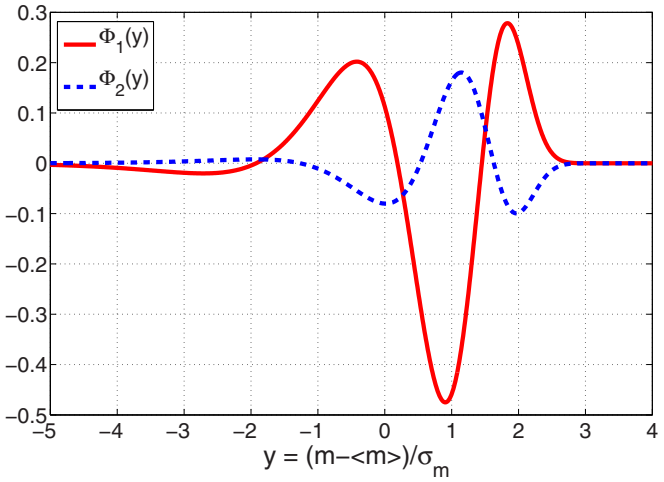

FIG. 2. Behavior of the scale-independent shape-correction functions $\Phi_1(y)$ and $\Phi_2(y)$.

there that the asymptotic L-dependence of δg_2 has the form $(C_1 \ln L + C_2)/L^2$ [cf. Eq. (A3)], while δg_n behaves as $\propto 1/L^2$ for $n > 2$ [cf. Eqs. (A8), (B4), and (B15)]. The result of these calculations is the amplitude of $\Phi_1(y)$ given by

$$a_1(L) = \frac{\alpha \ln L + \gamma}{L^2} = \frac{\alpha}{L^2} \ln \frac{L}{L_0}, \tag{26}$$

where the coefficient α is obtained analytically $\alpha = 3\pi/(4G) = 2.572\,361\,347\,6$, with G being the Catalan constant, while $\gamma = -2.802\,563\,265\,3$ and $L_0 = 2.972\,759\,081$ are determined numerically.

The amplitude $a_1(L)$ is the second main result of our work since the FS corrections are dominated by the $a_1(L)\Phi_1(y)$ term. Indeed, $a_2(L)/a_1(L)$ is small, 0.67, already for $L = 10$ and it decreases with increasing L. Furthermore, evaluating $\Phi_2(y)$ numerically, one finds that apart from the neighborhood of the zeros of $\Phi_1(y)$, the inequality $a_1(L)\Phi_1(y) \gg a_2(L)\Phi_2(y)$ holds for $L > 10$, as seen in Fig. 3.

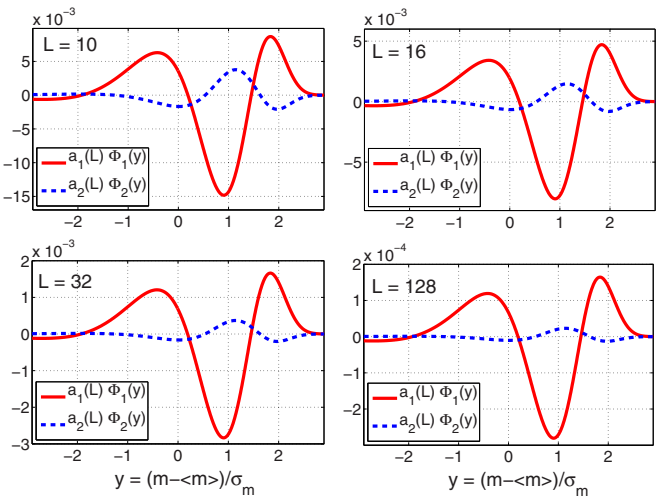

FIG. 3. Comparison of the two leading correction terms $a_1(L)\Phi_1(y)$ and $a_2(L)\Phi_2(y)$ for $L = 10$, 16, 32, and 128.

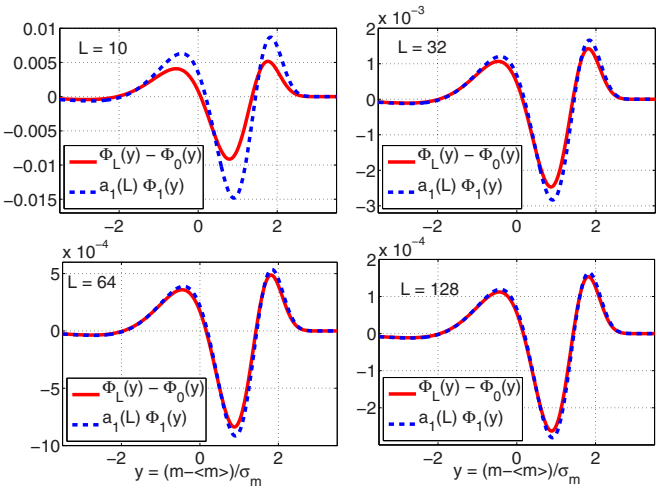

FIG. 4. Comparison of the exact FS correction $\Phi_L(y) - \Phi_0(y)$ with the leading term $a_1(L)\Phi_1(L)$ given by (25) and (26). Apart from the regions close to the maxima and minima, good agreement can be observed already for small system sizes.

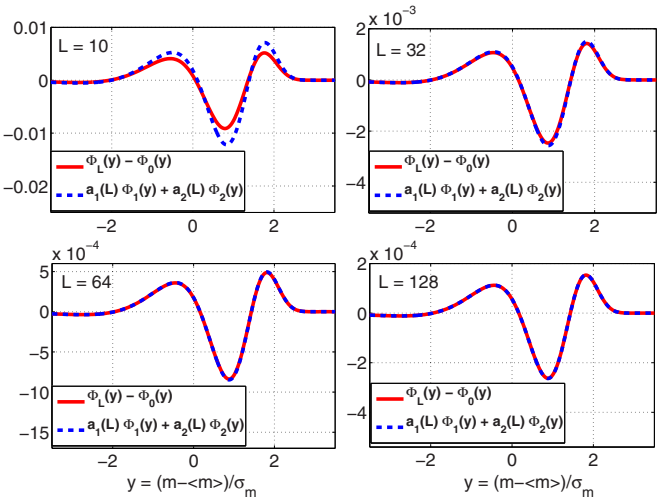

FIG. 5. Comparison of the exact FS correction $\Phi_L(y) - \Phi_0(y)$ with the leading terms $a_1(L)\Phi_1(L) + a_2(L)\Phi_2(y)$ for lattice sizes $L = 10$, 32, 64, and 128.

It should be mentioned that there is some freedom in separating the two contributions $a_1(L)\Phi_1(y)$ and $a_2(L)\Phi_2(y)$ in Eq. (2). One can replace $\Phi_2(y)$ with $\Phi_2(y) + c\Phi_1(y)$, changing simultaneously γ to $\gamma - c\gamma'$ in $a_1(L)$ [Eq. (20)]. Our choice of separating the leading large-n asymptote of δg_n in Eqs. (18) and (21) leads naturally to a function proportional to $\Phi_1(y)$ and also results in a remnant that is small already for small values of L. This choice is convenient, since it allows to write the FS correction in a compact form [see Eq. (5)] with a very good accuracy as demonstrated in Fig. 4.

It is remarkable that the dominant correction term $a_1(L)\Phi_1(y)$ also emerges from a simple assumption about the PDF written in its original variable. Namely, if we assume that one can write $P_L(m) = P_0(m) + \epsilon(L)P_0''(m)$, with $\epsilon \to 0$ for $L \to \infty$, we find that $\epsilon(L) = a_1(L)\,\sigma_m^2$. Using then the scaled variable y, the expression $\epsilon(L)P_0''(m)$ becomes $a_1(L)\Phi_1(y)$.

As discussed above, there are other choices for separating a contribution proportional to $\Phi_1(y)$. It should be clear, however, that the freedom is irrelevant when the sum of the two contributions $a_1(L)\Phi_1(y) + a_2(L)\Phi_2(y)$ is used. As expected, and as can be seen in Fig. 5, the convergence is fastest when the sum of both corrections are used.

IV. MONTE CARLO SIMULATIONS

Here we briefly demonstrate that the calculated FS corrections can be observed in simulations. It is clear that increasing the system size and improving the statistics by increasing the number of Monte Carlo samples, the leading FS corrections, as seen in Fig. 5, will emerge from the analysis. The question is whether the leading corrections we calculated could be seen already in small systems with reasonable simulation effort.

We have thus performed MC simulations on a 2D XY model of size $L = 10$ and computed $\Phi_L(y)$. Since our analytic results Eqs. (22)–(24) pertain to the $T = 0$ limit of the system, we made simulations deep in the low-T region ($T = 0.04$ and 0.02) using the overrelaxation Metropolis (ORM) algorithm [27]. In addition, simulations of the $T = 0$ limit itself could also be carried out since there the spin-wave approximation applies, which yields independent modes with Gaussian action whose simulation is straightforward [28].

In the simulation using ORM, we typically measured observables using 100×10^9 sweeps, and the errors were estimated by using a binning method. In Fig. 6, the red line shows the FS corrections to $\Phi_0(y)$ displayed as the difference $\Phi_{L=10}(y) - \Phi_0(y)$ computed from the integral representation of Eq. (9). It is compared with data obtained by ORM at very low temperatures $T = 0.04$ (green circles) and $T = 0.02$ (asterisk markers). The magenta points represent the results from the simulation of the Gaussian action at $T = 0$. The statistical errors on all the data points displayed are smaller than the point size, which is not surprising for the quoted large number of MC sweeps. From the actual statistical error $\sim 5 \times 10^{-5}$ one can find that a relatively small number, 3×10^8 sweeps are enough to reach an accuracy 10^{-3}, one-tenth of the maximal FS correction.

As one can see, the simulation temperatures used are small enough for the temperature corrections to be small compared to the FS corrections at $L = 10$. It can also be seen that the sum of the two leading FS correction terms, $a_1(L)\Phi_1(y) + a_2(L)\Phi_2(y)$ (blue dashed line), is quite close to the exact result. Of course, $L = 10$ is a rather small system to expect full agreement of the calculated leading FS corrections with the full FS correction. Looking at Fig. 5, however, one notes that increasing the size of the system by only a factor three would yield a complete domination of the leading FS corrections over the higher-order FS corrections.

Thus, we conclude that observing the leading FS corrections is feasible in relatively small systems at relatively small computational coast. Based on this observation, we expect that a meaningful analysis of FS corrections in experimental XY systems is also possible.

V. CONCLUSIONS

We have computed the leading FS corrections to the PDF of the magnetization of the 2D XY model at zero temperature.

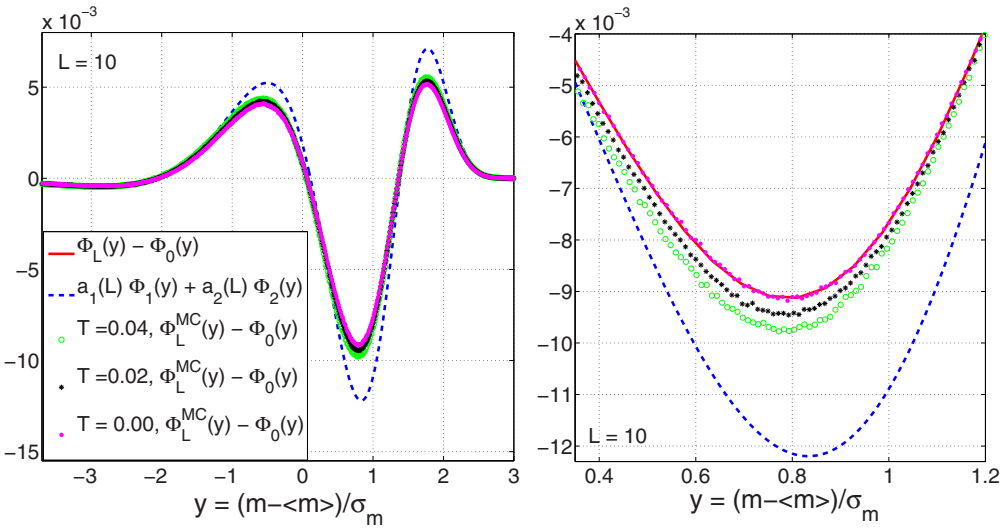

FIG. 6. Comparison of the exact FS correction $\Phi_L(y) - \Phi_0(y)$ (red line) and the leading terms $a_1(L)\Phi_1(L) + a_2(L)\Phi_2(y)$ (blue dashed line) with the MC simulations for lattice size $L = 10$. The region close to the minimum is magnified in the right panel. It shows that the ORM results approach $\Phi_L(y) - \Phi_0(y)$ as $T \to 0$.

Two scale-independent functions $\Phi_1(y)$ and $\Phi_2(y)$ were found with their amplitudes behaving with system size as $a_1(L) \sim \alpha \ln(L/L_0)/L^2$ and $a_2(L) \sim 1/L^2$. The function $\Phi_1(y)$ can be expressed through the limit distribution $\Phi_0(y)$ and its low-order derivatives. This makes it a candidate for identifying universality features hidden in FS corrections.

The leading and next-to-leading corrections were found to describe the FS behavior very accurately already for small system size. Thus, as our MC simulations demonstrated, the observation of the calculated FS corrections is possible in model systems. We expect that their experimental observation may also be feasible.

ACKNOWLEDGMENTS

This work was partially supported by Dicyt-USACH Grant No. 041531PA and PAI-CONICYT Grant No. 79140064 and by the Hungarian Research Fund (Grant No. OTKA NK100296). G.P. would like to thank the Institute for Theoretical Physics at Eötvös University, Budapest, for the invitation in the summer of 2014, where this collaboration started, and also thanks their members for kind hospitality.

APPENDIX A: FINITE-SIZE CORRECTIONS TO δg_n

We begin by deriving the large-L asymptotic expansion for g_2 defined in Eq. (10). It is convenient to write this equation in the form

$$g_2 = \frac{1}{(2\pi)^4} \sum_{l,m}{}' \left[l^2 + m^2 - \frac{1}{12}\left(\frac{2\pi}{L}\right)^2 (l^4 + m^4) + \cdots \right]^{-2}, \\ = g_2^{\infty} + \delta g_2, \tag{A1}$$

where the sum goes from $l,m = -L/2 + 1$, to $L/2$ and prime means that the $l = m = 0$ term is left out. The asymptotic value g_2^{∞} is given by

$$g_2^{\infty} = \frac{1}{(2\pi)^4} \sum_{l,m=-\infty}^{\infty}{}' \frac{1}{(l^2+m^2)^2} = G/(24\pi^2) \\ \approx 0.003\,866\,9, \tag{A2}$$

where G is Catalan's constant.

In the FS correction δg_2, the sum giving the coefficient of $1/L^2$ diverges logarithmically with L. This leading term is obtained as

$$\delta g_2 \sim \frac{1}{6(2\pi)^2 L^2} \sum_{l^2+m^2<L^2/4}{}' \frac{l^4+m^4}{(l^2+m^2)^3} + \cdots \\ = \frac{1}{6(2\pi)^2 L^2} \int_{1/L}^{1/2} \frac{dr}{r} \int_0^{2\pi} d\phi (\sin^4\phi + \cos^4\phi) + \cdots \\ = \frac{1}{16\pi} \frac{\ln L}{L^2} + O(L^{-2}). \tag{A3}$$

It is worthwhile mentioning that the $\ln L/L^2$ decay of δg_2 is consistent with the logarithmic FS corrections of some related quantities reported in [29].

The above expression for δg_2 can be generalized to perform a high-precision fit of the form

$$g_2(L) = g_2^{\infty} + \frac{1}{L^2}\left(\frac{1}{16\pi} \ln L + \gamma_2\right) \tag{A4}$$

to $g_2(L)$ computed numerically using Eq. (10) for a large range of L values [30].

In Fig. 7 we have plotted the numerically computed $g_2(L)$, as well as the FS scaling expression given by Eq. (A4). The value of the parameter $\gamma_2 = 0.003\,768\,763\,799$ was obtained from a high-precision fit over system sizes up to $L = 10^9$. In Appendix B we use a more sophisticated method to obtain an integral representation for γ_2 and found a complete agreement with the value cited above.

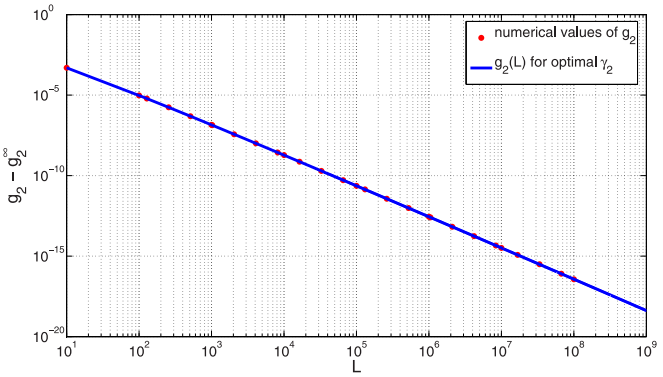

FIG. 7. Behavior of $g_2(L)$ as a function of lattice size L up to $L = 10^9$ in logarithmic scale. The red dots correspond to the direct numerical evaluation of Eq. (10) and the blue line corresponds to the analytic expression of Eq. (A4) for $\gamma_2 = 0.003\,768\,763\,799$.

Similarly to Eq. (A2), the asymptotic value g_n^∞ is given by

$$g_n^\infty = \frac{1}{(2\pi)^{2n}} {\sum_{l,m=-\infty}^{\infty}}' \frac{1}{(l^2+m^2)^n} = \frac{4}{(2\pi)^{2n}} \zeta(n)\beta(n), \tag{A5}$$

where $\zeta(n)$ and $\beta(n)$ are Riemann's ζ function and Dirichlet's β function, respectively [31].

For $n \geqslant 3$ the sum appearing in the $1/L^2$ correction term δg_n converges for $L \to \infty$; hence, one can extend the summation to $\pm\infty$ (up to an error decreasing faster than $1/L^2$). One has then

$$\frac{\delta g_n}{n g_n^\infty} = \frac{(2\pi)^2}{12L^2} \frac{\sum'_{l,m} (l^4+m^4)(l^2+m^2)^{-(n+1)}}{\sum_{l,m}' (l^2+m^2)^{-n}} = \frac{\pi^2}{3L^2}\left(1 + \frac{U_n}{V_n}\right), \tag{A6}$$

where

$$U_n = {\sum_{l,m}}' \frac{l^4 - l^2 + m^4 - m^2}{(l^2+m^2)^{n+1}}, \qquad V_n = {\sum_{l,m}}' (l^2+m^2)^{-n} = 4\zeta(n)\beta(n). \tag{A7}$$

For large n the dominant terms in these sums come from smallest $|l|, |m|$ with nonvanishing contributions. The numerator in U_n vanishes for the two shells $(l = \pm 1, m = 0)$, $(l = 0, m = \pm 1)$, and $(l = \pm 1, m = \pm 1)$. The leading term for large n is coming from $(l = \pm 2, m = 0)$ and $(l = 0, m = \pm 2)$ and is given by 12×4^{-n}. Since $V_n = 4(1 + 2^{-n} + \cdots)$ one finds that $U_n/V_n \sim 3 \times 4^{-n}$. This is a small correction; even for $n = 3$ it is just ≈ 0.047. Hence, we have, as stated in Eq. (18),

$$\frac{\delta g_n}{n g_n^\infty} = \frac{\pi^2}{3L^2} + \frac{1}{L^2} O(4^{-n}), \qquad n \geqslant 3. \tag{A8}$$

APPENDIX B: INTEGRAL REPRESENTATION FOR LEADING FINITE-SIZE CORRECTIONS

For calculating finite-volume sums for a cubic box of size L in d dimensions in the continuum, like ${\sum_{\mathbf{k}}}' 1/(\mathbf{k}^2)^n$, where $\mathbf{k}^2 = \sum_{i=1}^d (2\pi n_i/L)^2$, it is useful to introduce the function $S(x)$ (see, e.g., [32]) (related to Jacobi's θ function), defined as

$$S(x) = \sum_{n=-\infty}^{\infty} \exp(-\pi x n^2). \tag{B1}$$

It satisfies the relation

$$S(x) = \frac{1}{\sqrt{x}} S\left(\frac{1}{x}\right), \tag{B2}$$

which makes it possible to calculate $S(x)$ very precisely by taking only a few terms in the sum, for both $x < 1$ and $x > 1$. Note that $S(x) = x^{-1/2}[1 + 2\exp(-\pi/x) + \cdots]$ for $x \to 0$, while $S(x) = 1 + 2\exp(-\pi x) + \cdots$ for large x.

As an illustration, it is easy to show that g_n^∞ given by Eq. (A5) has an integral representation:

$$g_n^\infty = \frac{1}{(4\pi)^n \Gamma(n)} \int_0^\infty dx x^{n-1}[S^2(x) - 1]. \tag{B3}$$

The leading term for $n \to \infty$ is given by the large-x behavior of the integrand. Separating it, one obtains an expression,

$$g_n^\infty = \frac{4}{(2\pi)^{2n}} + \frac{1}{(4\pi)^n \Gamma(n)} \times \int_0^\infty dx x^{n-1}[S^2(x) - 1 - 4e^{-\pi x}], \tag{B4}$$

which can be evaluated and shown to be in agreement with Eq. (A5). With the help of this one can perform the summation in Eq. (15), yielding

$$F_0(k) = \int_0^\infty \frac{du}{2u}[S^2(uw) - 1] \times \left\{ e^{iku} - \left(1 + iku - \frac{1}{2}k^2u^2\right)\right\}, \tag{B5}$$

where $w = 4\pi\sqrt{g_2^\infty/2}$. The Fourier transformation appearing here can be performed efficiently by a fast Fourier transform (FFT).

This technique can be generalized to finite-volume lattice sums by introducing [33]

$$Q_L(z) = \frac{1}{L}\sum_{l=0}^{L-1} \exp\left(-z\hat{k}_l^2\right) = \phi_0(z) + 2\sum_{m=1}^{\infty} \phi_{mL}(z), \tag{B6}$$

where $\hat{k}_l^2 = 2[1 - \cos(2\pi l/L)]$, $l = 0, \ldots, L-1$, and

$$\phi_n(z) = e^{-2z} I_n(2z), \tag{B7}$$

with $I_n(z)$ being the modified Bessel function. For large z one has $\phi_0(z) \sim 1/\sqrt{4\pi z}$.

For fixed z with increasing L the function $Q_L(z)$ approaches $\phi_0(z)$ exponentially fast. The convergence becomes slower with increasing z, but even when the argument increases slower than L^2 one still has

$$\lim_{L\to\infty}[Q_L(cL^\alpha)-\phi_0(cL^\alpha)]=0 \qquad \text{for } \alpha<2, \tag{B8}$$

with the difference decreasing faster than any inverse power of L. This is not true for $z\propto L^2$, and for this case one obtains another scaling function. Rescaling $Q_L(z)$, we introduce the lattice counterpart [33] of $S(x)$ by

$$S_L(x)=LQ_L\left(\frac{xL^2}{4\pi}\right). \tag{B9}$$

By expanding Eq. (B6) for large L one finds the asymptotic expansion

$$S_L(x)=S(x)+\frac{\pi}{3L^2}xS''(x)+O\left(\frac{1}{x^2L^4}\right). \tag{B10}$$

As the error term indicates, the approach to $L=\infty$ is not uniform in x.

Using $S_L(x)$ one has for $g_n=g_n(L)$ two integral representations:

$$\begin{aligned} g_n&=\frac{L^{-2n+2}}{\Gamma(n)}\int_0^\infty dzz^{n-1}\left[Q_L^2(z)-\frac{1}{L^2}\right]\\ &=\frac{1}{(4\pi)^n\Gamma(n)}\int_0^\infty dxx^{n-1}\left[S_L^2(x)-1\right]. \end{aligned} \tag{B11}$$

We outline below the calculation of δg_2 to $O(1/L^2)$. Due to the nonuniform convergence for $L\to\infty$ it is useful to split the integration region and write

$$\begin{aligned} g_2(L)&=\frac{1}{L^2}\int_0^{z_0}dzz\left[Q_L^2(z)-\frac{1}{L^2}\right]\\ &\quad+\frac{1}{(4\pi)^2}\int_{x_0}^\infty dxx\left[S_L^2(x)-1\right], \end{aligned} \tag{B12}$$

where $x_0=4\pi z_0/L^2$. Choosing $z_0=z_0(L)=cL^{2-\epsilon}$ with some fixed small $\epsilon>0$ in the first term, one could replace $Q_L(z)$ with $\phi_0(z)$ up to exponentially small corrections. Similarly, in the second integral one can use the expansion Eq. (B10). Note that $z_0(L)\to\infty$ and $x_0(L)\to 0$ for $L\to\infty$. Using Eq. (B10) and neglecting terms vanishing faster than $1/L^2$, one obtains

$$\delta g_2=\frac{1}{L^2}\int_0^{z_0}dzz\phi_0^2(z)+\frac{2\pi}{3L^2(4\pi)^2}\int_{x_0}^\infty dxx^2S(x)S''(x). \tag{B13}$$

Separating the asymptotic behavior of the integrands for large z and small x, respectively, one obtains the logarithmic contribution $1/(32\pi)\ln(z_0/x_0)=1/(16\pi)\ln L$, and in the remaining terms one can make the substitutions $z_0=\infty$ and $x_0=0$. Evaluating the corresponding integrals, one reproduces the fit result Eq. (A4) to all digits (cf. Fig. 7).

The leading correction of δg_n for $n>2$ is simpler and given by the convergent integral

$$\delta g_n=\frac{2\pi}{3L^2}\frac{1}{(4\pi)^n\Gamma(n)}\int_0^\infty dxx^nS(x)S''(x), \quad n\geqslant 3. \tag{B14}$$

Separating the large-x term of the integrand, one obtains

$$\begin{aligned} \delta g_n&=\frac{\pi^2}{3L^2}\frac{4n}{(2\pi)^{2n}}+\frac{2\pi}{3L^2}\frac{1}{(4\pi)^n\Gamma(n)}\\ &\quad\times\int_0^\infty dxx^n[S(x)S''(x)-2\pi^2e^{-\pi x}], \end{aligned} \tag{B15}$$

where $n\geqslant 3$. The leading term has the same form as for ng_n^∞ [cf. Eq. (B4)]. Subtracting this way the leading term, one can define c_n by

$$\delta g_n=\frac{\pi^2}{3L^2}ng_n^\infty+\frac{2\pi}{3L^2}c_n, \tag{B16}$$

where for $n\geqslant 3$:

$$c_n=\frac{1}{(4\pi)^n\Gamma(n)}\int_0^\infty dxx^nS(x)[S''(x)+\pi S'(x)]. \tag{B17}$$

For large n one has $c_n\sim 6\pi n(4\pi)^{-2n}$; i.e., it is suppressed by a factor of 4^{-n} compared to ng_n^∞.

Inserting Eq. (B17) into Eq. (21) we obtain an integral representation for $\Psi_2(k)$:

$$\begin{aligned} \Psi_2(k)&=\frac{w}{2}\int_0^\infty duS(uw)\{S''(uw)+\pi S'(uw)\}\\ &\quad\times\left[e^{iku}-\left(1+iku-\frac{1}{2}k^2u^2\right)\right]. \end{aligned} \tag{B18}$$

Using FFT one can evaluate this and finally the corresponding correction $\Phi_2(y)$ to the PDF.

[1] M. E. Fisher, Critical Phenomena, in *Proceedings of the 1970 International School of Physics "Enrico Fermi", Course LI*, edited by M. S. Green (Academic, New York, 1971).

[2] J. L. Cardy, *Finite Size Scaling* (North-Holland, Amsterdam, 1988).

[3] Edited by V. Privman, *Finite Size Scaling and Numerical Simulation of Statistical Physics* (World Scientific, Singapore, 1990).

[4] A. D. Bruce, J. Phys. C **14**, 3667 (1981).

[5] K. Binder, Z. Phys. B **43**, 119 (1981).

[6] D. Nicolaides and A. D. Bruce, J. Phys. A **21**, 233 (1988).

[7] Examples of wide-ranging applications are A. D. Bruce and N. B. Wilding, Phys. Rev. Lett. **68**, 193 (1992) (liquid-gas transition); D. Nicolaides and R. Ewans, *ibid.* **63**, 778 (1989) (wetting); N. B. Wilding and P. Nielaba, Phys. Rev. E **53**, 926 (1996) (tricritical point); M. Müller and N. B. Wilding, *ibid.* **51**, 2079 (1995) (polymers); S. L. A. de Queiroz and R. B. Stinchcombe, *ibid.* **64**, 036117 (2001) (random-field Ising

model); M. M. Tsypin, Phys. Rev. Lett. **73**, 2015 (1994) (field theory).

[8] G. Foltin, K. Oerding, Z. Rácz, R. L. Workman, and R. K. P. Zia, Phys. Rev. E **50**, R639 (1994); Z. Rácz and M. Plischke, *ibid.* **50**, 3530 (1994); E. Marinari, A. Pagnani, G. Parisi, and Z. Rácz, *ibid.* **65**, 026136 (2002).

[9] S. T. Bramwell, P. C. W. Holdsworth, and J.-F. Pinton, Nature (London) **396**, 552 (1998); J.-F. Pinton, P. C. W. Holdsworth, and R. Labbé, Phys. Rev. E **60**, R2452(R) (1999).

[10] V. Aji and N. Goldenfeld, Phys. Rev. Lett. **86**, 1007 (2001); N. Soulopoulos, Y. Hardalupas, and A. M. K. P. Taylor, Phys. Fluids **27**, 125103 (2015).

[11] S. T. Bramwell, K. Christensen, J.-Y. Fortin, P. C. W. Holdsworth, H. J. Jensen, S. Lise, J. M. López, M. Nicodemi, J. F. Pinton, and M. Sellitto, Phys. Rev. Lett. **84**, 3744 (2000).

[12] G. Korniss, Z. Toroczkai, M. A. Novotny, and P. A. Rikvold, Phys. Rev. Lett. **84**, 1351 (2000); S. Lubeck and P. C. Heger, *ibid.* **90**, 230601 (2003); T. Halpin-Healy and G. Palasantzas, Europhys. Lett. **105**, 50001 (2014); X. Clotet, S. Santucci, and J. Ortin, Phys. Rev. E **93**, 012150 (2016).

[13] J. M. Kosterlitz and D. J. Thouless, J. Phys. C **6**, 1181 (1973).

[14] P. M. Chaikin and T. C. Lubensky, *Principles of Condensed Matter Physics* (Cambridge University Press, Cambridge, UK, 1996).

[15] T. Tóth-Katona and J. T. Gleeson, Phys. Rev. Lett. **91**, 264501 (2003); S. Joubaud, A. Petrosyan, S. Ciliberto, and N. B. Garnier, *ibid.* **100**, 180601 (2008); I. Jánossy, K. Fodor-Csorba, A. Vajda, and T. Tóth-Katona, Phys. Rev. E **89**, 012504 (2014).

[16] S. T. Bramwell, T. Fennel, P. C. W. Holdsworth, and B. Portelli, Europhys. Lett. **57**, 310 (2002); K. Dahlstedt and H. Jensen, Phys. A (Amsterdam, Neth.) **348**, 596 (2005).

[17] S. F. Edwards and D. R. Wilkinson, Proc. R. Soc. London, Ser. A **381**, 17 (1982).

[18] S. T. Bramwell, J.-Y. Fortin, P. C. W. Holdsworth, S. Peysson, J.-F. Pinton, B. Portelli, and M. Sellitto, Phys. Rev. E **63**, 041106 (2001).

[19] S. T. Bramwell, Nat. Phys. **5**, 444 (2009).

[20] G. Mack, G. Palma, and L. Vergara, Phys. Rev. E **72**, 026119 (2005).

[21] G. Palma, Phys. Rev. E **73**, 046130 (2006).

[22] S. T. Banks and S. T. Bramwell, J. Phys. A **38**, 5603 (2005).

[23] T. Antal, M. Droz, G. Györgyi, and Z. Rácz, Phys. Rev. Lett. **87**, 240601 (2001); Phys. Rev. E **65**, 046140 (2002).

[24] P. Archambault, S. T. Bramwell, J.-Y. Fortin, P. C. W. Holdsworth, S. Peysson, and J.-F. Pinton, J. Appl. Phys. **83**, 7234 (1998).

[25] G. Jona-Lasinio, Phys. Rep. **352**, 439 (2001).

[26] J. Cardy, *Scaling and Renormalization in Statistical Physics* (Cambridge University Press, Cambridge, UK, 1996).

[27] M. Creutz, Phys. Rev. D **36**, 515 (1987); K. Kanki, D. Loison, and K. D. Schotte, Eur. Phys. J. B **44**, 309 (2005).

[28] Integrating out the Gaussian variables one obtains the analytic expression in Eq. (9).

[29] R. Kenna and A. C. Irving, Phys. Lett. B **351**, 273 (1995); W. Janke, Phys. Rev. B **55**, 3580 (1997); S. G. Chung, *ibid.* **60**, 11761 (1999).

[30] Note that in the double sum appearing in (10) the summation over one of the integers can be done analytically, which makes possible to reach large values of L.

[31] See, e.g., I. S. Gradstein and I. M. Ryshik, *Table of Integral Series and Products*, 7th ed. (Elsevier Academic, San Diego, 2007).

[32] P. Hasenfratz and H. Leutwyler, Nucl. Phys. B **343**, 241 (1990).

[33] F. Niedermayer and P. Weisz, J. High Energy Phys. 06 (2016) 102.